Nuclear Engineering and Technology 48 (2016) 1423–1432

Available online at ScienceDirect

Nuclear Engineering and Technology

journal homepage: www.elsevier.com/locate/net

Original Article

Application of the French Codes to the Pressurized Thermal Shocks Assessment

Mingya Chen [a,*], Guian Qian [b], Jinhua Shi [c], Rongshan Wang [a], Weiwei Yu [a], Feng Lu [a], Guodong Zhang [a], Fei Xue [a], and Zhilin Chen [a]

[a] Suzhou Nuclear Power Research Institute, Life Management Center, Xihuan Road, 215004, Suzhou, Jiangsu Province, PR China

[b] Paul Scherrer Institute, Nuclear Energy and Safety Department, Laboratory for Nuclear Materials, OHSA/06, 5232, Villigen PSI, Switzerland

[c] Amec Foster Wheeler, Clean Energy Department, 19B Brighouse Court, Barnett Way, Gloucester GL2 4NF, UK

ARTICLE INFO

Article history:
Received 17 March 2016
Received in revised form
18 May 2016
Accepted 3 June 2016
Available online 30 June 2016

Keywords:
Pressurized Thermal Shock
RCC-M
Reactor Pressure Vessel
RSE-M
Structural Integrity

ABSTRACT

The integrity of a reactor pressure vessel (RPV) related to pressurized thermal shocks (PTSs) has been extensively studied. This paper introduces an integrity assessment of an RPV subjected to a PTS transient based on the French codes. In the USA, the "screening criterion" for maximum allowable embrittlement of RPV material is developed based on the probabilistic fracture mechanics. However, in the French RCC-M and RSE-M codes, which are developed based on the deterministic fracture mechanics, there is no "screening criterion". In this paper, the methodology in the RCC-M and RSE-M codes, which are used for PTS analysis, are firstly discussed. The bases of the French codes are compared with ASME and FAVOR codes. A case study is also presented. The results show that the method in the RCC-M code that accounts for the influence of cladding on the stress intensity factor (SIF) may be nonconservative. The SIF almost doubles if the weld residual stress is considered. The approaches included in the codes differ in many aspects, which may result in significant differences in the assessment results. Therefore, homogenization of the codes in the long time operation of nuclear power plants is needed.

1. Introduction

The reactor pressure vessel (RPV) is a key component of nuclear power plants (NPPs) with regard to safety and lifetime [1]. Although long time operation (LTO) is a main concern, the pressurized thermal shock (PTS) event poses a potentially significant challenge to the structural integrity of the RPV [2]. Prior to 1978, it was postulated that the most severe PTS event was a large-break loss-of-coolant accident (LOCA). During that type of overcooling transient, low-temperature emergency coolant would rapidly enter and cool the vessel wall which would result in high thermal stresses. In 1978, the occurrence

* Corresponding author.
E-mail addresses: chenmingya@cgnpc.com.cn, p134362@163.com (M. Chen).
http://dx.doi.org/10.1016/j.net.2016.06.009

of an event at the Rancho Seco NPP in the USA showed that rapid cool-down could be accompanied by repressurization during some types of overcooling transients. Following the incident, the USA Nuclear Regulatory Commission (NRC) designated PTS as an unresolved safety issue, and the effects of PTS were extensively analyzed [3]. On the basis of those analyses, the NRC established the Regulatory Guide (RG) 1.154 [4] and 10 Code of Federal Regulation (CFR) 50.61 [5] rules. The 10 CFR 50.61 establishes a "screening criterion" based on the reactor vessel nil-ductility-transition temperature (RT_{NDT}). The screening criterion RT_{NDT} (called RT_{PTS} in the rule) was selected according to the studies that the risk due to PTS events is acceptable based on the probabilistic fracture mechanics (PFM). In 10 CFR 50.61, the RT_{PTS} is 132°C for plates, forgings, and axial welds, and 149°C for circumferential welds. As long as the limiting temperature is not reached, the risk caused by the PTS events is considered to be acceptable. The PTS issues are widely studied in the USA. However, the technical basis of FAVOR, which is developed by Oak Ridge National Laboratory (ORNL) in Washington, DC and used by the US NRC to perform the PTS analysis [6–8], is not consistent with other codes and standards, such as the ASME [9], RCC-M [10], and RSE-M [11] codes.

Furthermore, no such "screening criterion" exists in the French codes, e.g., RCC-M and RSE-M which were developed based on the deterministic fracture mechanics (DFM). The RPV assessment is mainly based on simplified methods ("engineering approach") instead of the more sophisticated approach in these codes. The criteria of the Level C "exceptional conditions" and Level D "highly improbable conditions", which may be classified as the PTS transients, are lacking clear descriptions. In addition, some fracture mechanics inputs, such as the thermal and stress analyses, have not been revisited since their original design. Therefore, it may be difficult to reassess the safety of the RPV under PTS loadings during the LTO operation according to the RCC-M and RSE-M codes. In fact, there is only a small amount of literature based on the RCC-M or RSE-M codes to assess RPV integrity, even though the resistance of RPV against fast fracture has been comprehensively studied.

This paper aims to apply the French codes, RCC-M and RSE-M, to perform an RPV integrity assessment, to compare the two codes with the ASME codes, and to discuss the limitations of the three codes. In this paper, the methodology of the Level C and Level D in the French codes, which is classified as the PTS assessment, is firstly discussed. Meanwhile, the methodology is further compared with the fundamental of the FAVOR software. A case study according to the RCC-M and RSE-M codes is presented. Lastly, the limitations of the RCC-M and RSE-M codes, as well as the important factors for the RPV structural assessment, i.e., weld residual stress, cladding influence, and crack arrest assessment criteria, are discussed.

1.1. *PTS assessment procedure*

The PTS assessment of RPV integrity is based on comparisons of crack driving forces (such as stress intensity factor, SIF K_I) calculated for assessed points along the crack front with its allowable value (such as fracture toughness K_{IC}) for PTS events [12,13]. The flowchart of the PTS analysis is shown in Fig. 1, and the main evaluations are described in the following steps: (1) prediction of material toughness according to the chemical compositions, initial toughness, neutron fluence and material embrittlement; (2) calculation of PTS transients according to thermal-hydraulic analysis; (3) analyses of thermal-mechanical and welding residual stress; (4) definition crack information (position, orientation, size, and type): perform fracture mechanics analysis to calculate the SIF of the postulated cracks; (5) definition failure criteria according to the code (failure model and margin); and (6) assessment: compare SIFs of the postulated cracks with the failure criteria (fracture toughness of the embrittled material).

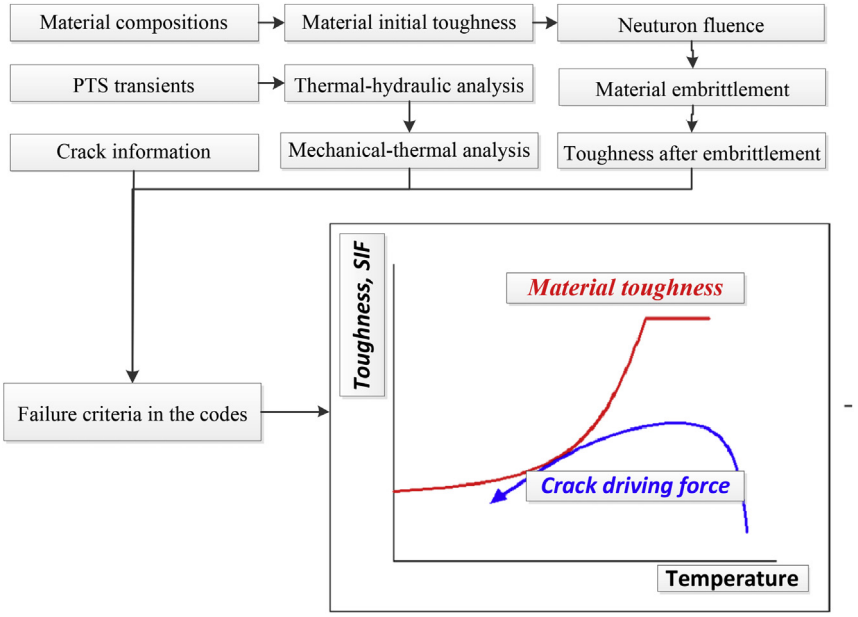

Fig. 1 – Diagrammatic representation of the PTS analysis. PTS, pressurized thermal shock; SIF, stress intensity factor.

In the following, the material property, e.g., material toughness and irradiation embrittlement, PTS transient calculation, crack models, and assessment criteria will be discussed.

2. Materials and methods

2.1. Material properties

2.1.1. Material toughness

As described above, material toughness is the critical material property in the PTS study. For ferritic steels, the static fracture toughness $K_{IC}(\mathrm{MPa}\cdot\sqrt{\mathrm{m}})$ and the crack arrest toughness $K_{Ia}(\mathrm{MPa}\cdot\sqrt{\mathrm{m}})$ are functions of the material temperature $T(^{\circ}\mathrm{C})$ and RT_{NDT} (°C) in the RCC-M and RSE-M codes. In the RSE-M code Version 2007, the toughness is defined as follows:

$$K_{IC} = \min\{36.5 + 3.1\exp[0.36(T - RT_{NDT} + 55.5)], 220\} \quad (1a)$$

$$K_{Ia} = \min\{29.43 + 1.355\exp[0.0261(T - RT_{NDT} + 88.9)], 220\} \quad (1b)$$

It is well known that the weld zone includes the parent, the weld, and the heat affected zone (HAZ). In actual structural assessments, the equation above may be used for all materials, while the RT_{NDT} is calculated according to different materials. In the USA, it is recommended and considered adequately conservative to use the equation for steels of minimum yield strengths up to and including 345 MPa [14]. In the early 2000s, it became clear that the irradiation effect on the weld metal of Ringhals 3 and 4 in Swedish reactors was different to that in Westinghouse type RPVs.

As shown in Eq. (1), the upper shelf values of K_{IC} and K_{Ia} have no relationship with the neutron fluence. Although the upper shelf value can be taken as 200 $\mathrm{MPa}\cdot\sqrt{\mathrm{m}}$ in [15], 240 $\mathrm{MPa}\cdot\sqrt{\mathrm{m}}$ is implicitly endorsed by the ASME code [9]. In the USA, Appendix G of 10 CFR 50 [16] requires the upper shelf energy throughout the life of the vessel to be no less than 67.8 J which implicitly endorses that the upper shelf values are related to the fluence. However, there is no description in the RCC-M and RSE-M codes about the relationship between the upper shelf energy and the neutron fluence. This needs further improvement.

2.1.2. Irradiation embrittlement of the RPV

RPV material tends to embrittle due to neutron irradiation and the degree of embrittlement is quantified by the change in RT_{NDT} in the RCC-M and RSE-M codes. The final RT_{NDT} is obtained by adding the shift (ΔRT_{NDT}) to the initial value. The following equation is used in the RCC-M Version 2007, Appendix Z G for the base metal 16MND5:

$$\Delta RT_{NDT} = [22 + 556(\%Cu - 0.08) + 2778(\%P - 0.008)]\left(f/10^{19}\right)^{1/2}, \quad (2)$$

in which, %Cu and %P represents the weight-percent measured values of Cu and P. f represents the fluence expressed in neutrons per cm^2, where only neutrons having energy > 1 MeV are considered.

In the RSE-M code Version 2010, the shift of the RT_{NDT} due to the embrittlement can be calculated according to the RCC-M code, or calculated according to the Fragilisation par Irradiation Superieure (FIS) equation:

$$\Delta RT_{NDT} = 15.4\{1 + 35.7\max[0; (P - 0.008)] + 6.6\max[0, (Cu - 0.08)] + 5.8Ni^2Cu\}\phi^{0.59} \quad (3)$$

in which, P, Cu, and Ni represent the weight-percent measured values of P, Cu, and Ni. ϕ represents the fluence expressed in neutrons per cm^2, where only neutrons having energy > 1 MeV are considered.

The FIS equation is based on research by Brillaud, where a series of French surveillance data was analyzed [17]. Compared with the RCC-M code, the influence of Ni composition is considered in the FIS equation. The initial design values of the maximum fluence level from AREVA were between 5.1 and $5.6 \times 10^{19} n/\mathrm{cm}^2$ (E > 1MeV) for the design life of 40 years. The reevaluation in 2001 led to $7.2–7.6 \times 10^{19} n/\mathrm{cm}^2$ (E > 1 MeV) projected for 40 years. The FIS equation is only applicable up to a maximum neutron fluence of $11.5 \times 10^{19} n/\mathrm{cm}^2$ (E > 1 MeV). Thus, during the LTO (operate to 60 years), the fluence will be close to the limit of the equations.

2.2. PTS transient calculation

PTS transients are significant in terms of the stresses which are likely to be induced with associated temperatures, and the temperatures impact on the toughness of the material. The output of the thermal hydraulic analysis, which is input into the fracture mechanics model, is the temporal variation of pressure, temperature, and heat transfer coefficients (HTCs) along the RPV downcomer.

In the design stage, the temporal variation of pressure and temperature at the inlet nozzle of RPVs is given while the focused area is the beltline region in the PTS assessment. The RPV is approximated by a rotationally symmetric two-dimensional model that allows the calculation of axial and circumferential stresses as a function of one-dimensional (along the radial direction) transient temperature distribution [18]. For the simplified analysis in the design stage, the forced convection or free convection of HTCs are often used. In the PTS assessment, some countries adopt the view that the thermal plumes that can occur below the cold legs are of sufficiently small magnitude that they can be neglected, while other countries directly model the effect of these plumes. In the latter case, the pressure, temperature, and HTCs variation along the downcomer takes on both a spatial and a temporal variation [19,20].

In the ASME Code Section XI Appendix E, the pressure and temperature are the temporal variation, and the HTCs should be considered under the event, plant specific flow, and mixing conditions. However, there are few descriptions concerning the thermal-hydraulic calculation in the RCC-M and RSE-M codes.

2.3. Crack models

In PTS analysis, it is necessary to demonstrate that the integrity criteria are satisfied for the postulated defects located at the beltline region with high neutron fluence. However, the postulation of a defect is problematic. The inner

surface of the RPVs is protected with as austenitic cladding to prevent corrosion. Cladding materials are characterized by relatively lower toughness in comparison with the same austenitic material that is not austenized after welding. The cladding is heat treated to remove residual stresses [15]. In the design stage of the RCC-M code, the cladding may be taken into account in determining the temperature and stress fields, but should be neglected for the fracture analyses [10].

In the RCC-M code Version 2010, the conventional reference defect is shown in Fig. 2, and the flaw depth a is defined as follow:

$$a = \min(0.25t,\ 20mm) \quad t > 40mm \tag{4}$$

in which, t is the thickness of the vessel, $2b$ is the flaw length and $a/2b = 1/6$.

The postulated defects are assumed to be normal to the direction of the maximum principal stresses. For semi-elliptical inner-surface-breaking defects, both the deepest point (DP, point A in Fig. 2) on the crack front and the edge located at the intersurface (IP, point B) should be analyzed. Defects smaller than the reference defect must also be analyzed to ensure that they are no more severe.

The flaw information of the RSE-M code is in accordance with the actual nondestructive examination (NDT) information. The flaw depth a is defined as the sum of the actual crack size and the margin. It is known that no flaws in base metal extended up to the inner surface of the RPV are found in real cladded RPVs [21]. Fracture toughness of the first layer of cladding is important for potential arrest of the underclad crack propagation. If the crack is not arrested there, the second layer of cladding has low fracture toughness and cannot arrest [22,23]. On the basis of these results, a new type of postulated underclad crack for PTS calculations is included in the RSE-M code Version 2007, as shown in Fig. 3 (the first layer is close to the base, and the second layer is close to the inner surface of the RPV). For a circumferential or longitudinal continuous subclad crack of height $h = 2a$, whose extremity A is located in the cladding and extremity B in the base metal, the equivalent SIF is calculated at the crack tip points A and B, which implicitly endorses that both ends of the defects must be analyzed in the RSE-M code. Thus, the fracture toughness value of the cladding is needed, whereas there is no description in the RSE-M code [23,24].

In the USA, the ASME Code Section XI App. E "Evaluation of Unanticipated Operating Events" [9] provides acceptance

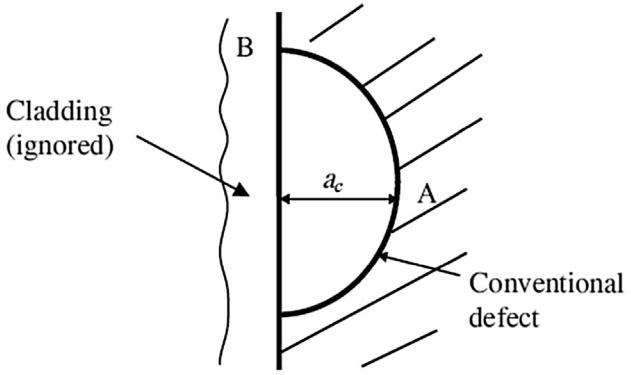

Fig. 2 – Conventional reference defect in RCC-M code.

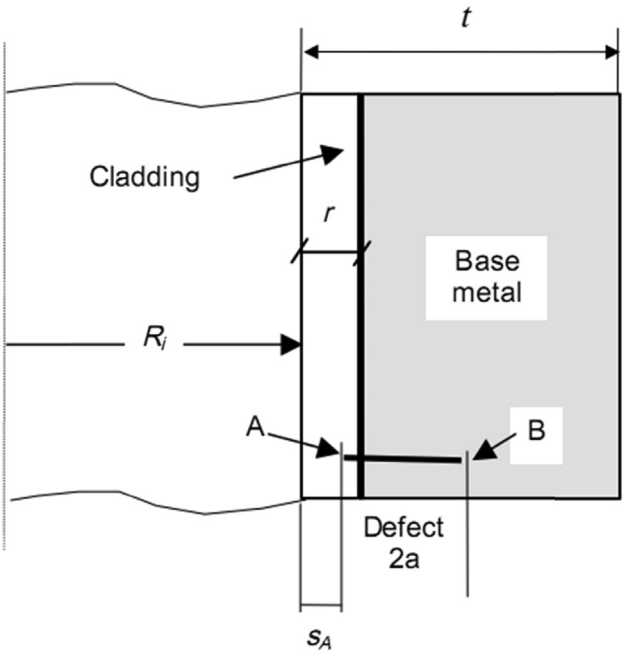

Fig. 3 – Conventional subcladding crack in RSE-M code. r, the thickness of the cladding; S_A, ligament between the internal surface of the vessel and extremity A of the crack.

criteria and guidance for performing an engineering evaluation on the effects of PTS on the structural integrity of the RPV beltline region. In App. E which is based on the DFM, a semi-elliptical surface flaw is used, and cladding should be considered in the thermal, stress and fracture mechanics analyses.

The flaw information in FAVOR is in accordance with the actual NDT information. The surface-breaking flaws only exist in the cladding in the FAVOR, which means that there is no embedded flaw propagating through the cladding. This is same in the RSE-M code, but obviously different to the hypothesis in the RCC-M and ASME codes. The models in the RCC-M and ASME codes conservatively postulate that all flaws are inner-surface-breaking flaws. In the reference [12–14,22], the SIF of the subclad crack may be 50% lower than that of the surface breaking crack.

2.4. *Assessment criteria*

In the RCC-M and RSE-M codes, the information which may be used for PTS assessment, is contained in the Level C "Exceptional conditions" and Level D "Highly improbable conditions". In the RCC-M code Version 2007 and RSE-M code Version 2005, the criteria for Level C and Level D are given in Table 1.

As shown in Table 1, only crack initiation assessment is considered in the transient region ($T \le RT_{NDT} + 60°C$), while cracks which initiate in the cool inner region of the vessel may be arrested in a region of the wall where temperature is much higher and neutron fluence is lower [13,15]. Thus, the focusing of RCC-M and RSE-M codes on the beltline region is a conservative assumption. In a ductile tearing analysis for the high temperature range ($T \ge RT_{NDT} + 40°C$), the crack shape parameter $a/2b$ is kept at 1/6 in the RCC-M code while the

Table 1 – Criteria in the RCC-M and RSE-M codes.[a]

		RCC-M		RSE-M	
		Level C	Level D	Level C	Level D
$T \le RT_{NDT} + 60°C$		$K_{CP} \le K_{IC}/1.6$	$K_{CP} \le K_{IC}/1.2$	$K_{cp}(1.3C_C) \le \min(K_{IC}/1.35, K_{JC}/1.25)$	$K_{cp}(1.3C_D) \le \min(K_{IC}/1.35, K_{JC}/1.25)$
$T \ge RT_{NDT} + 40°C$	Option 1	$K_{CP} \le K_{JC}/1.3$	$K_{CP} \le K_{JC}/1.0$	$J(1.3C_C) \le J_{0.2}$	$J(1.1C_D) \le J_{0.2}$
	Option 2	$K_{CP} \le K_{JC}/1.1$ with a margin of 1.6 on ductile tearing	a margin of 1.2 is verified against ductile tearing	$J(1.3C_C) \le J_{\Delta a}/1.6$ and $J(1.3C_C) \le J_{0.2}$	$J(1.3C_D) \le J_{\Delta a}/1.1$

[a] K_{CP} is the total SIF including plastic correction, T is the material temperature at the point in time and at the point on the crack front under analysis, C_C and C_D mean the loads of Level C and Level D events, and K_{JC} is the material toughness indicated by static measurements of J_{IC}. SIF, stress intensity factor.

crack is expected to be of an infinite length after initiation in the RSE-M code.

The margin is only applied on the material toughness in the RCC-M code. By contrast, margins are applied both on the toughness and the crack driving forces in the RSE-M code. The question is how to apply the margin on the crack driving forces, such as the thermal stress and residual stress in the three-dimensional finite element analysis (FEA). However, there is no clear description of the criteria in the codes. Thus, it may be difficult to carry out the assessment according to the RSE-M code.

The criterion in the ASME Code Sec. XI App. E is as follow.

$$1.4(K_{IM} + K_{It}) + K_{Ir} \le K_{IC} \quad (5)$$

where K_{IM} is the SIF due to membrane stress, K_{It} is the SIF due to thermal stress, and K_{Ir} is the SIF due to residual stress.

According to Eq. (5), it implicitly endorses that the margin is applied on the SIF due to membrane stress and thermal stress in the ASME code, and only crack initiation assessment is required while crack arrest assessment is an option in the RCC-M and RSE-M codes. The residual stress is considered in the ASME code but not considered in the RCC-M and RSE-M codes.

It should be pointed out that both the RCC-M and RSE-M codes are based on DFM, while the screening criterion of the USA is based on PFM. The main differences among these codes are listed in Table 2.

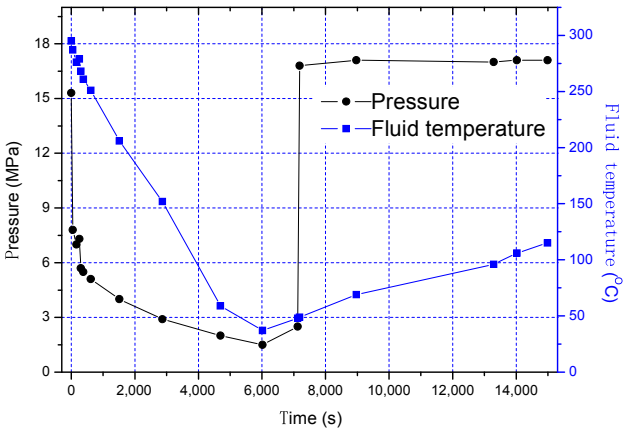

Fig. 4 – Pressure–temperature versus time in the IAEA report. IEA, International Atomic Energy Agency.

3. Case study

The example documented in the International Atomic Energy Agency (IAEA) report [15] is used to illustrate the detailed methodology and results according to the French codes. The time variations of pressure and fluid temperature around the beltline are shown in Fig. 4, and the HTCs are shown in Table 3.

Table 2 – Compare the guidelines in different codes.

		RCC-M	RSE-M	USA criteria
Crack	Size	Min (1/4 thickness, 20 mm)	Measured + uncertainties	Probabilistic
	Type	Surface	Real and subsurface	Subsurface for the base metal crack
	Location	Beltline and nozzle	Real, beltline, and nozzle	Beltline
	Orientation	Longitudinal	Circumferential or longitudinal	Circumferential or longitudinal
Cladding		Not considered in fracture assessment	Considered	Considered
Ductile tearing		Yes	Yes	Only after arrest
Thermal analysis		Simplified analysis	Exact analysis	Exact analysis by RELAP 5 software
Failure criteria	Model	Initiation and ductile tearing	Initiation and ductile tearing	Initiation and ductile tearing after arrest
	Margin	On toughness	On force and toughness	No
Residual stress		Not considered	Not considered	Considered
DFM or PFM		DFM	DFM	PFM

DFM, deterministic fracture mechanics; PFM, probabilistic fracture mechanics.

Table 3 – HTCs around the beltline.

Temperature/°C	37	48	49	59	69	96	106	115	152
HTCs/(W/(m^2·°C))	992	877	790	1,147	602	710	1,229	1,057	1,838
Temperature/°C	206	251	261	268	276	279	287	295	/
HTCs/W/(m^2·°C)	1,581	4,834	1,757	6,232	3,453	1,054	24,696	24,125	/

HTC, heat transfer coefficients.

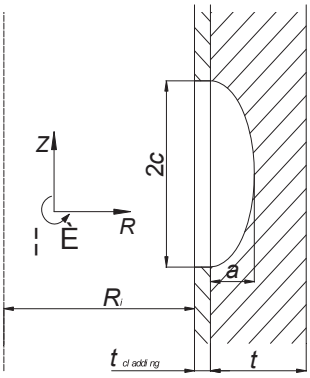

Fig. 5 – The postulated crack model in the core region of the RPV. RPV, reactor pressure vessel.

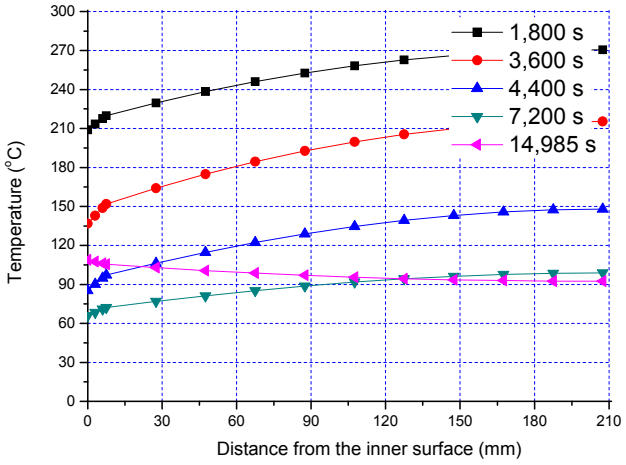

Fig. 6 – The temperature field at different stages of the transient.

As shown in Fig. 5, the inner radius of the RPV R_i is 1994 mm, the thickness of the base metal t is 200 mm and the thickness of cladding $t_{cladding}$ is 7.5 mm, respectively [15]. The inner side of the RPV is assumed to be subjected to thermal shocks, and the thermal load is assumed to be rotationally symmetric and homogeneous along the Z-axis in the analysis. The beltline region of the RPV is sufficiently far away from the nozzle area to be treated as axisymmetric cylindrical shell.

The RPV was modeled with SA508 Class 3 steel and the cladding was made of austenitic stainless steel, respectively. Temperature dependent material properties used in the analyses are summarized in Table 4 [15].

4. Results

4.1. *Temperature and stress distributions*

The temperature distribution through the vessel wall at different times of the transient is shown in Fig. 6. Due to rapid cooling, the temperature difference along the vessel wall increases in the beginning of the transients. As the temperature of the coolant is no longer fluctuant, isothermal conditions are achieved in the vessel wall at the end stage of the transient.

The elastic hoop stress in the PTS transient is shown in Fig. 7. The discontinuity of the stress in the clad-base metal interface is due to the different properties of the cladding and base materials. The higher thermal expansion coefficient and the lower thermal conductivity of the cladding are responsible for the increased stress in the cladding zone (reaching the yield stress). Due to the reduced temperature gradient, the thermal stress starts unloading in the end stage.

4.2. *Crack driving force K_{CP}*

The SIF is determined from the defect size under consideration, its position, and the associated stresses under analysis. This determination may be performed in accordance with the following procedure in the RCC-M code: (1) determination the distribution of stresses caused by all applied loads at the point in the time under consideration. The stress fit is carried out

Table 4 – Material properties of the base metal and cladding.

Material	Temperature (°C)	Young modulus/E (GPa)	Poisson's rationν	Thermal conductivity [W/(m·°C)]	Thermal diffusivity$\mu = \lambda/\rho C$ (10^{-6} m^2/s)	Density (10^3kg/m^3)	Coefficient of thermal expansion[a] (10^{-6}/°C)	Yield stress (MPa)
Base metal	20	204	0.3	54.6	14.7	7.6	10.9	588
	300	185		45.8	10.6		12.9	517
Cladding	20	197	0.3	14.7	4.1	7.6	16.4	380
	300	176.5		18.6	4.3		17.7	270

[a] Mean value between 20°C and the temperature.

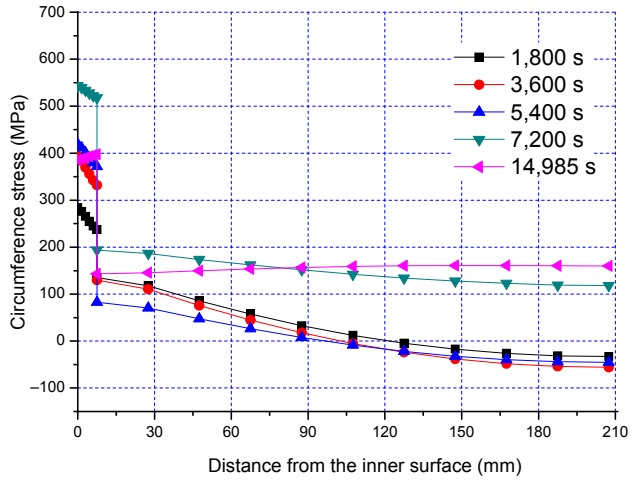

Fig. 7 – The elastic hoop stress in the PTS transient. PTS, pressurized thermal shocks.

over a distance part L of the wall thickness of the studied zone, and only by taking into account the stresses normal to the postulated defect plane. The distribution of normal stress $\sigma(x)$ is fitted by a polynomial with variable x:

$$\sigma(x) = \sigma_0 + \sigma_1(x/L) + \sigma_2(x/L)^2 + \sigma_3(x/L)^3 + \sigma_4(x/L)^4 \quad (6)$$

where x is the distance to the wall $0 \le x \le t$ if t is the thickness of the studied zone. L is the distance over which the stress is expressed by the polynomial: $0 \le L \le t$; (2) determination the SIF K_I by associating an influence function to each term in the polynomial expression. Influence functions are represented by i_0, i_1, i_2, and i_3, and are the function of crack geometry, the zone in which the postulated crack is located, and the a/L ratio. The K_I is expressed as follows, and the influence functions are given in RCC-M Z G 5120:

$$K_I = (\pi a)^{1/2}\left(\sigma_0 i_0 + \sigma_1(a/L)i_1 + \sigma_2(a/L)^2 i_2 + \sigma_3(a/L)^3 i_3\right) \quad (7)$$

and (3) correction of the plastic zone must be applied according to the following procedure. Determine the radius r_y of the plastic zone at the defect tip, as follows:

$$r_y = \frac{1}{6\pi}\left(\frac{K_I}{\sigma_y}\right)^2 \quad (8)$$

where σ_y is the yield strength value for the material at the crack tip at the temperature of the point in time considered. Determine the corrected value of the intensity factor K_{CP} as follows:

$$K_{CP} = \alpha K_I\sqrt{(a + r_y)/a} \quad (9)$$

in which,

$$\alpha = 1, \text{ if } r_y \le 0.05(t - a) \quad (10a)$$

$$\alpha = 1 + 0.15\left[\frac{r_y - 0.05(t-a)}{0.035(t-a)}\right]^2, \text{ if } 0.05(t-a) < r_y \le 0.12(t-a) \quad (10b)$$

$$\alpha = 1.6, \text{ if } r_y > 0.12(t - a) \quad (10c)$$

in which, α is the additional plasticity correction in order to take into account cladding yielding.

In reality, the method used to calculate K_{CP} is based on the plane strain conditions in the RCC-M code which is implicitly endorsed in the Z G 5220 "Determination of crack-extension force J". In the Z G 5220, J may be computed from K_{CP} using the following equations:

$$J = (1 - \nu^2)K_{CP}^2/E, \text{ at DP} \quad (11a)$$

$$J = K_{CP}^2/E, \text{ at IP} \quad (11b)$$

The plan strain assumption in the calculation of SIF for the IP is conservative according to the RCC-M code. The assessment of SIF for the point of intersection of the crack front with the free surface could also be performed by other more sophisticated methods, which take into account the plane stress conditions in this point.

In the RCC-M code Version 2007, the maximum flaw depth a is min (0.25t, 20 mm), and $2b/a = 6$ (defects smaller than the maximum defect which must also be analyzed are not assessed in this case study). The temporal variation of the stress fields caused by the thermal and pressure loads are used to calculate the SIF. The results according to the RCC-M code are shown in Table 5, and they are also compared to the results of the 3-D FEA. The detailed methods of the 3-D FEA are described in reference [2,8,13]. The FEA was carried out using the general-purpose FEA program ABAQUS, Version 6.12, and only one quarter of the beltline was modeled considering symmetric conditions. The hexahedron element is used, and the pressure load on the crack surface was considered for the through-clad defect.

As shown in Table 5, the method to account for the influence of cladding on the SIF is nonconservative in the RCC-M code. As in the previous analysis, the stress in the cladding region is higher than the yield stress, so the influence of the cladding on the SIF is obvious. In this case study, the radius r_y at the crack tip is always smaller than 0.05(t-a), this means that the influence of the cladding is actually ignored. Nevertheless, according to the FEA study, the influence of the cladding on SIF is obvious.

In the elastic–plastic analyses, the stress within the cladding will be limited, if the plasticity is incorporated, so the K_{CP} values may be smaller than K_I for the DP [13]. While in the RCC-M code, the plasticity correction always increases the SIF.

Table 5 – SIF results at time 7,200 s of the transient.

Location	K_I(MPa·$\sqrt{\text{m}}$)		K_{CP}(MPa·$\sqrt{\text{m}}$)	
	RCC-M code	3-D FEA	RCC-M code[a]	3-D FEA
DP	47.11	67.68	47.56	67.16
IP	30.67	68.78	30.78	85.17

[a] Yield stress at crack tip temperatures is determined by the linear interpolation.
SIF, stress intensity factor.

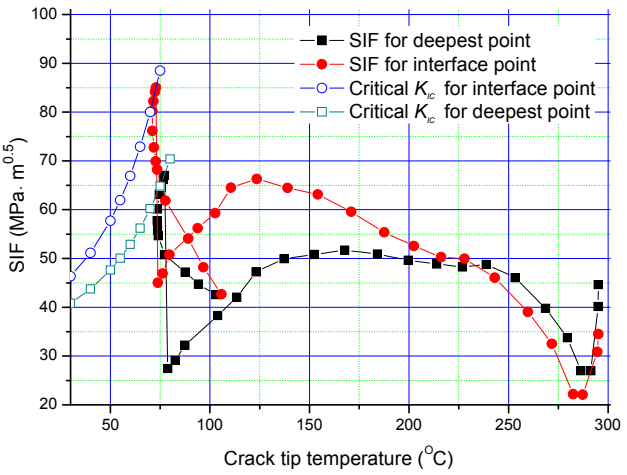

Fig. 8 – Elastic-plastic SIF and the safety assessment. SIF, stress intensity factor.

4.3. *Safety assessment*

The critical crack tip temperature is much lower than RT_{NDT} + 60°C in the IAEA report. Therefore, according to the RCC-M code, the failure criterion is as follow:

$$K_{CP} \leq K_{IC}/1.6 \quad (12)$$

The relationship between elastic-plastic SIF and crack tip temperature, calculated by the FEA method, is shown in Fig. 8. The maximum allowable RT_{NDT} is also calculated based on the tangent method. Due to the influence of the cladding, the IP is more dangerous than the DP in the case study (the plane strain conditions are defined for all points).

As shown in Fig. 8, the critical moment of fracture may not coincide with the time to get the maximum SIF, as the crack tip temperature may be higher at that time. Consequently, there may be a set of moments in which the safety assessment needs to be performed, according to the RCC-M code. The results of the safety assessment at time of 7,200 s, based on the RCC-M code, are shown in Table 6. The allowed critical value of RT_{NDT} is only about 52°C for the DP which is much lower than the "screening criterion" of the USA. The main difference is due to the fact that the "screening criterion" is determined by a probabilistic approach, different flaws, different methods for considering cladding, safety margins, and failure criteria.

4.4. *Discussion*

4.4.1. *Effect of weld residual stress*

Residual stress is not considered in the RCC-M and RSE-M codes, and the influence of the residual stress on the SIF of the circumferential surface-break cracks in the circumferential weld of the RPV beltline is shown in Table 7. The stress free temperature (SFT) is chosen to be 295°C and the default residual stress in the FAVOR is used in the study.

As shown in Table 7, the SIF increases about 18% after the residual stress through-wall distribution is considered, indicating that the influence of the residual stress cannot be ignored.

4.4.2. *Effect of cladding*

As the SIF of the subclad crack may be 50% lower than that of the surface breaking crack [12–14], the influence of the cladding is particularly significant on the safety margin, since the existence of cladding decreases the SIF significantly and consequently increases the maximum allowable RT_{NDT}.

SFT is used to consider the influence of the residual stress caused by the cladding in the FAVOR code. The SIF results of the DPs, with and without the influence of the weld residual stress caused by the cladding, are shown in Table 8. As shown in Table 8, the SIF increases significantly if the cladding residual stress is considered, and the SIF almost doubles when the crack size is small. This indicates that the influence of the cladding residual stress cannot be ignored. However, there is little material data on the cladding and there is also no description of it in the RCC-M and RSE-M codes. Therefore, the material data of the

Table 6 – Safety assessment results.

Location	K_{CP}(MPa·$\sqrt{m}$)	Crack tip temperature (°C)	Allowed critical value of RT_{NDT} (°C)		
			Based on RCC-M method	Based on 3-D FEA	In the IAEA report[a]
DP	47.56	66.58	52.02	69.9	57.5
IP	30.78	76.86	93.26	52.8	77.9

[a] The results of AREVA in the IAEA report are used. The distance of IP from the interface is 2 mm in the IAEA report. Also, the smaller crack (crack depth a = 12 mm) is postulated in the IAEA report.
DP, deepest point; IAEA, International Atomic Energy Agency; IP, interface point.

Table 7 – SIF results with and without the residual stress.

Residual stress	a = 6 mm, $a/2b$ = 1/6	a = 6 mm, $a/2b$ = 0	a = 12 mm, $a/2b$ = 1/6	a = 12 mm, $a/2b$ = 0	a = 24 mm, $a/2b$ = 1/6	a = 24 mm, $a/2b$ = 0
Not considered	42.45	49.90	45.93	53.61	48.72	57.85
Considered	50.28	58.57	54.57	63.72	57.67	69.13
Increment (%)	18.45	17.37	18.81	18.86	18.37	19.50

SIF, stress intensity factor.

Table 8 – SIF results of DPs with and without the cladding residual stress.

SFT (°C)	$a = 6$ mm, $a/2\ b = 1/6$	$a = 6$ mm, $a/2b = 0$	$a = 12$ mm, $a/2b = 1/6$	$a = 12$ mm, $a/2b = 0$	$a = 24$ mm, $a/2b = 1/6$	$a = 24$ mm, $a/2b = 0$
20	26.70	26.11	32.30	33.67	41.28	45.46
295	42.45	49.90	45.93	53.61	48.72	57.85
Increment (%)	58.99	91.11	42.20	59.22	18.02	27.25

DP, deepest point, SIF, stress intensity factor.

cladding, such as the fracture toughness and weld residual stress, need to be defined in any future PTS assessment.

In the above analyses, the cladding is considered in the models. It was assumed that the cladding always bears the loads along with the base material during the PTS transients. In reality, there may be many small cracks in the cladding and the near surface crack is hard for the NDT to detect during the service period. According to the RSE-M and ASME codes, there is no need to assess the cracks which are located in the cladding region. Neglecting of the cracks embedded in the cladding is a conservative assumption.

When the cladding loses the strength to bear the loads (map cracking, MC) before PTS transient occurs, the MC effect on fracture analysis should be considered. In this case, the cladding may conduct heat flux but lose the strength to bear the loads during PTS transients. Fig. 9 shows the maximum thermal stress SIF with or without considering the MC effect under different cool-down rates [2]. When the MC effect is considered, the thermal stress SIF reduces obviously. The decrement of IPs is much larger than that of DPs. The MC effect means to release the constraints on the flaw, especially for the IPs.

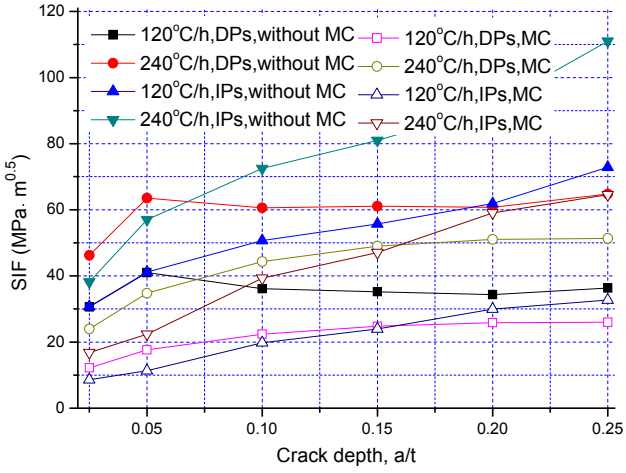

Fig. 9 – Influence of the MC on the peak thermal stress SIF. IP, interface point; MC, map cracking; SIF, stress intensity factor.

Table 9 – SIF of different crack shape parameters.

		$a = 10$ mm	$a = 20$ mm	$a = 40$ mm
$a/2b = 1/6$	DP	63.67	67.68	81.58
	IP	52.79	68.78	90.18
$a/2b = 0$		88.89	101.84	138.20

DP, deepest point; IP, interface point; SIF, stress intensity factor.

4.4.3. *Crack arrest and ductile tearing assessments*

As shown in Table 1, only crack initiation assessment is considered during the transient period, according to RCC-M and RSE-M codes. By contrast, crack arrest assessment has been considered in the FAVOR code [6]. Concerning crack arrest, RCC-M and RSE-M codes are more conservative.

In the ductile tearing analysis in the high temperature region, the crack shape parameter $a/2b$ is kept at 1/6 in the RCC-M code, while the crack shape parameter is expected to be zero (infinite) after crack initiation in the RSE-M code. In addition, the safety margin of IP may be smaller than that of DP [3,8]. However, there are few published papers that showed the differences among different codes, which may puzzle the user [25]. The SIFs at time of 7,200 s of the transient for the inner surface break cracks with different shape parameters are shown in Table 9. The comparison of SIFs shows that the criteria in the RSE-M code is more conservative than that in the RCC-M code.

5. Conclusion

Based on this study, the following conclusions can be drawn: (1) in the PTS assessment of RP, the approaches in RCC-M, RSE-M and ASME codes differs in many aspects, including flaw size, the role of cladding, safety margins, and failure criteria. The difference will result in different assessment results. Thus, the codes need to be homogenized concerning weld residual stress, cladding influence and the exact safety assessment criteria in the LTO of NPPs; (2) the method in the RCC-M code to account for the influence of cladding on the SIF is nonconservative. Neglecting the weld residual stress in the French codes leads to nonconservative results in the structural integrity assessment, but there are many factors influencing the assessment results which need to be studied in future work; and (3) the influence of the cladding on RPV integrity is significant. The material data of the cladding, such as the fracture toughness and weld residual stress, should be provided in the assessment. In order to perform a more realistic integrity assessment for the LTO of NPPs, accurate thermal analysis and exact crack arrest assessment criteria are needed.

Conflicts of interest

All authors have no conflicts of interest to declare.

Acknowledgments

The project is supported by the National Natural Science Foundation of China (No. 51275338 and No. 51435012). The

financial supports of both programs are greatly appreciated. We are also indebted to Mr. Terry Dickson of the Oak Ridge National Laboratory for providing the code FAVOR.

REFERENCES

[1] G.A. Qian, M. Niffenegger, Investigation on constraint effect of a reactor pressure vessel subjected to pressurized thermal shocks, Jour. Pre. Ves. Tec 137 (2015) 1–7.
[2] M.Y. Chen, F. Lv, R.S. Wang, P. Huang, X.B. Liu, G.D. Zhang, The deterministic structural integrity assessment of reactor pressure vessels under pressurized thermal shock loading, Nucl. Eng. Des 288 (2015) 84–91.
[3] W.E. Pennell, Structural integrity assessment of aging nuclear reactor pressure vessels, Nucl. Eng. Des 172 (1997) 27–47.
[4] US Nuclear Regulatory Commission, Format and Content of Plant-specific Pressurized Thermal Shock Safety Analysis Reports for Pressurized Water Reactors, Washington, D.C., 1987. Regulatory Guide, No. 1.154
[5] US Nuclear Regulatory Commission, Fracture Toughness Requirements for Protection Against Pressurized Thermal Shock Events, US Nuclear Regulatory Commission, Washington, D.C., 1984, 10 CFR 50.61.
[6] Oak Ridge National Laboratory, Fracture Analysis of Vessels—Oak Ridge FAVOR, v06.1, Computer Code: Theory and Implementation of Algorithms, Methods and Correlations, Oak Ridge National Laboratory, Washington, D.C., 2006.
[7] P. Vladislav, M. Pota, D. Lauerova, Probabilistic assessment of pressurised thermal shock, Nucl. Eng. Des 272 (2013) 84–91.
[8] M.Y. Chen, F. Lv, R.S. Wang, W.W. Yu, The probabilistic structural integrity assessment of reactor pressure vessels under pressurized thermal shock loading, Nucl. Eng. Des 294 (2015) 93–102.
[9] American Society of Mechanical Engineers, ASME Boiler and Pressure Vessel Code, Section XI, Appendix E, Evaluation of unanticipated operating events, American Society of Mechanical Engineers, New York, NY, 2013.
[10] RCC-M. Design and construction for mechanical components of PWR nuclear island, Sec. I. Subsec. Z. Annex Z G, Fast Fracture Resistance, French association for design, construction and in-service inspection rules for nuclear island components, Paris, 2010.
[11] RSE-M, In-service Inspection Rules for the Mechanical Components of PWR Nuclear Islands, French association for design, construction and in-service inspection rules for nuclear island components, Paris, 2007.
[12] Y.B. He, T. Isozaki, Fracture mechanics analysis and evaluation for the RPV of the Chinese Qinshan 300 MW NPP under PTS, Nucl. Eng. Des 201 (2000) 121–137.
[13] M.Y. Chen, F. Lv, R.S. Wang, Structural integrity assessment of the reactor pressure vessel under the pressurized thermal shock loading, Nucl. Eng. Des 272 (2014) 84–91.
[14] US Welding Research Council, Recommendations on Toughness Requirements for Ferritic Materials, US Welding Research Council, Washington, D.C., 1972.
[15] International Atomic Energy Agency, Pressurized Thermal Shock in Nuclear Power Plants: Good Practices for Assessments, International Atomic Energy Agency, Vienna, 2010. IAEA-TECDOC-1627.
[16] US Nuclear Regulatory Commission, Fracture Toughness Requirements, 10 CFR 50 Appendix G, US Nuclear Regulatory Commission, Washington, D.C., 1984.
[17] F. Lu, R.S. Wang, P. Huang, H.Y. Qian, Prediction of irradiation embrittlement for Chinese domestic A508-3 steel, in: Proceedings of the 18th International Conference on Nuclear Engineering. Beijing, 2010.
[18] G.A. Qian, M. Niffenegger, Procedures, methods, and computer codes for the probabilistic assessment of reactor pressure vessels subjected to pressurized thermal shocks, Nucl. Eng. Des 258 (2013) 35–50.
[19] M. Scheuerer, J. Weis, Transient computational fluid dynamics analysis of emergency core cooling injection at natural circulation conditions, Nucl. Eng. Des 253 (2012) 343–350.
[20] J.P. Fontes, C. Raynaud, A. Martin, Reactor pressure vessel: EDF R&D program to support lifetime management, in: Pressure Vessels & Piping Conference, 2011, pp. 1–5.
[21] T.L. Dickson, J.A. Keeney, J.W. Bryson, Validation of a linear-elastic fracture methodology for postulated flaws embedded in the wall of a nuclear reactor pressure vessel, in: Proceedings of ASME Pressure Vessel and Pipings, Seattle, 2000.
[22] D. Moinereau, G. Bezdikian, C. Faidy, Methodology for the pressurized thermal shock evaluation: recent improvement in French RPV PTS assessment, Int. J. Pres. Ves. Pip 78 (2001) 69–83.
[23] M. Brumovsky, M. Kytka, R. Kopriva, Cladding in RPV integrity and lifetime evaluation, in: 14th International Conference on Pressure Vessel Technology, 2015, pp. 1–10.
[24] J.S. Lee, I.S. Kimi, C.H. Jang, A. Kimura, Irradiation embrittlement of cladding and HZA of RPV steel, Nucl. Eng. Tech 38 (2005) 405–410.
[25] H. Churiep, G. Balard, E. Meister, F. Clemendot, P. Todeschini, French nuclear reactor pressure vessel integrity assessment and life management strategy, in: Pressure Vessels & Piping Conference, 2011, pp. 1–6.